Article

Characterization of Water-Resistant Adhesive Prepared by Cross-Linking Reaction of Oxidized Starch with Lignin

Chengyuan Liu , Huali Lin , Shichao Zhang , Hisham Essawy , Hongyan Wang , Longxu Wu , Xinyi Chen , Xiaojian Zhou , Antonios N. Papadopoulos * , Antonio Pizzi * , Ming Cao *

Posted Date: 12 May 2025

doi: 10.20944/preprints202505.0760.v1

Keywords: lignin; soy protein; oxidation; crosslinking reaction; wood adhesive

 doi:10.20944/preprints202505.0760.v1

Article

Characterization of Water-Resistant Adhesive Prepared by Cross-Linking Reaction of Oxidized Starch with Lignin

Chengyuan Liu [1,2,†], Huali Lin [1,2,†], Shichao Zhang [1,2], Hisham Essawy [3], Hongyan Wang [4], Longxu Wu [5], Xinyi Chen [1,2], Xiaojian Zhou [1,2], Antonios N. Papadopoulos [6], Antonio Pizzi and Ming Cao [1,2,*]

[1] Yunnan Provincial key laboratory of wood adhesives and glued products, College of Material and Chemical Engineering, Southwest Forestry University, Kunming 650224, China
[2] International Joint Research Center for Biomass Material, Southwest Forestry University, Ministry of Science and Technology, Kunming 650224, China
[3] Department of Polymers and Pigments, National Research Centre, Cairo 12622, Egypt
[4] Zhejiang Academy of Forestry, Hangzhou, Zhejiang, China
[5] College of Forestry, Guizhou University, Guiyang 550025, China
[6] Department of Natural Environment and Climate Resilience Sciences, Democritus University of Thrace, Drama-Mikrochoriou, 66100, Drama-Greece
[7] University of Lorraine, Epinal Cedex 9, France
* Correspondence: antpap@neclir.duth.gr (A.N.P.) ; antonio.pizzi@univ-lorraine.fr (A.P.); caoming__happy@126.com (M.C.)
† These authors contributed equally to this work.

Abstract: Wood adhesives play a critical role in the wood processing industry; however, traditional formaldehyde-based adhesives pose health risks and are reliant on non-renewable resources. This study aims to develop a bio-based wood adhesive with excellent water resistance, focusing on environmentally friendly solutions. The synthesis of an oxidized starch-lignin (OSTL) composite adhesive was accomplished by modifying starch via oxidation (ST) and subsequent cross-linking with lignin. Ammonium persulfate (APS) was employed for oxidation of starch, introducing aldehyde groups that upgrade its reactivity with lignin. Subsequently, the oxidized starch (OST) was cross-linked with the phenolic rings of lignin, resulting in a strong network structure. The oxidation of starch and its cross-linking mechanism with lignin were investigated using FT-IR, 1H-NMR, and XPS techniques, proving the formation of aldehyde and carboxyl groups with subsequent reaction possibilities.The effects of oxidant dosage, oxidation time, and the ratio of OST to lignin on the adhesive properties were systematically studied. The results demonstrated that the OSTL adhesive, prepared under optimized conditions, exhibited outstanding adhesion strength and water resistance in both dry and wet states, significantly outperforming conventional wood adhesives in terms of cold water, hot water, and boiling water resistance. In addition, the thermal behavior of the OSTL adhesive was further validated using differential scanning calorimetry (DSC) as well as thermogravimetric analysis (TGA). This study presents new insights and technical support for the development of green, environmentally friendly, and highly water-resistant lignin-based bio-adhesives.

Keywords: lignin; soy protein; oxidation; crosslinking reaction; wood adhesive

 doi:10.20944/preprints202505.0760.v1

1. Introduction

Wood adhesives play a crucial role in wood processing industry. The most widely used wood adhesives are formaldehyde-based resin adhesives, including phenolic resin, urea-formaldehyde resin, and melamine-formaldehyde resin, which account for over 90% of the market share in the industry [1]. However, formaldehyde-based resin adhesives release free formaldehyde, which poses health risks, with another shortcoming that their production relies on non-renewable petroleum resources. With the tightening of environmental regulations and the increase in consumer environmental awareness, eco-friendly biomass wood adhesives have developed rapidly [2]. Examples include lignin-based adhesives, tannin-based adhesives, and soy protein-based adhesives.

Lignin is the second largest biomass resource in the world. The total annual production of natural lignin can reach 1.5×10^{11} tons, while the by-products of industrial lignin produced annually in the pulp and paper industries can reach 6×10^{10} tons [3]. However, the utilization rate of lignin is currently low, with only a small portion being effectively utilized. Lignin is a high-molecular-weight compound with a three-dimensional polyphenolic network structure, making it the largest biomass alternative to petroleum-based aromatic materials. Additionally, lignin plays a role in plant cell structures by linking cellulose and hemicellulose to support the cell wall, thus imparting certain adhesive properties and strength. Due to its structural characteristics, lignin has great potential as an adhesive [4]. However, lignin-based adhesives face challenges such as poor water resistance, low bonding strength, and short storage life, which significantly limits their applications. Many researchers are using lignin either partially or entirely as a substitute for fossil-based materials to address the formaldehyde emissions associated with phenol-formaldehyde resins in adhesives. Sarkar et al. [5] used dealkalized lignin to replace 50% of phenol in phenol-formaldehyde resins, resulting in lignin-modified phenol-formaldehyde resins (LPF) with adhesive performance reaching 78% of pure phenol-formaldehyde resin. Sudan et al. [6], after alkali-based phenolation modification of lignin extracted from black liquor, were able to replace 60% of phenol, producing high-performance LPF resin. Bornstein et al. [7] heated lignin extracted from sulfite pulp waste liquor with formaldehyde under alkaline conditions, then added a small amount of melamine to produce a water-resistant wood adhesive. The adhesive contained up to 70% lignosulfonate, and significantly reduced the emission of free formaldehyde. These studies indeed demonstrated the strategy of using lignin to modify formaldehyde-based resin adhesives, which is not only more environmentally friendly and efficient but also established important foundations for the development of new bio-based adhesives. The use of lignin to modify formaldehyde-based adhesives can actually improve the bonding performance and reduce some formaldehyde emissions. However, it still requires the use of formaldehyde and does not fundamentally solve the formaldehyde emission problem. Therefore, many researchers explored the potential use of petroleum-based aldehydes such as propionaldehyde [8], glutaraldehyde [9], and glyoxal [10] to replace formaldehyde. Comparatively, ethylene glycol has lower toxicity[11]. Also, using some non-toxic, green biomass aldehydes as alternatives to formaldehyde in adhesives preparation helps mitigate the issue of formaldehyde emission currently faced. Some studies focused on the use of lignin to replace a part of the phenol and then completely substituted formaldehyde with ethylene glycol in adhesives preparation. This approach resulted in adhesives exhibiting higher bonding performance than PF resin adhesives [12,13]. Furthermore, adding petroleum-based cross-linking agents to lignin-ethylene glycol resin was reported to enhance the adhesive's bonding strength [7,8]. There are also studies [14] on adding hexamethylenetetramine as hardener to lignin-ethylene glycol resin, to cause improving of the adhesives dry shear strength up to 1.40 MPa. However, these cross-linking modifiers are expensive, leading to high production costs and limited economic benefits. Additionally, they still contain toxic substances. To address these issues, many groups opted to use furfural, lignin derivatives (such as hydroxybenzaldehydes, vanillin, syringaldehyde, and eugenol), as well as some non-toxic, green biomass aldehydes like sugar aldehydes, all of which can substitute formaldehyde in adhesive formulations. Zhang [15] and Dongre [16], among others, utilized hydrolyzed lignin and hydroxymethyl furfural to prepare lignin-furfural adhesives, achieving a high yield of 85%. Its

 doi:10.20944/preprints202505.0760.v1

functional groups and curing mechanism are similar to phenol-formaldehyde resins. Moreover, it showed a larger molecular weight, broader molecular weight distribution, and higher glass transition temperature, storage modulus, and tensile strength compared to phenol-formaldehyde resins. Compared to PF adhesives, the curing of lignin-furfural adhesives required higher curing temperatures and long curing times. Therefore, lignin-furfural adhesives still cannot meet the industrial requirements in relation to the curing speed and temperature. Furthermore, to enhance the lignin activity, phenol pretreatment of lignin is sometimes an option, but this approach does not fully achieve the greenification of adhesives.

Natural green sugar-based materials such as starch, sucrose, glucose, and cellulose are widely utilized for their sustainability and high biodegradability, especially in the bio-materials field, serving as an excellent feed-stock for sugar based aldehydes. In a previous research work belonging to our group, oxidized sucrose-lignin adhesive was prepared by achieving cross-linking between the oxidized sucrose with lignin. After immersing the adhesive-bonded three-layer plywood in hot water at 63 ± 3°C for 3 hours, the shear strength reached 1.42 MPa. In addition, the shear strength of the plywood samples after immersion in boiling water for 3 hours achieved 1.03 MPa. This approach replaces formaldehyde with oxidized sucrose, addressing the issue of toxic formaldehyde emissions while maintaining excellent performance.

Starch is an abundant, inexpensive natural polymer [17–20]. However, it has low reactivity and typically requires chemical or physical modification for optimal application. It consists of two main components: amylose and amylopectin [21]. The ratio of amylose to amylopectin significantly affects the physical and chemical properties of starch and its applications [22]. Some studies explained that starch with higher amylose content often produces harder gels and more robust films [23]. Therefore, the current study will focus on utilization of soluble amylose-rich starch as a raw material for preparation of bio-aldehydes.

The high functionalization of starch is related to its abundant hydroxyl groups on the molecular chains of sugar-based backbone, which can be easily chemically modified. Among suggested modifications, oxidation is one of the most common chemical treatments. After oxidation, the hydroxyl groups on starch molecules can directly upgrade to carbonyl or carboxyl groups along the molecular structure on the pretext that the hydroxyl groups at positions C2, C3, and C6 of the molecular structure of sugar-based materials are the most susceptible sites for oxidation agents to attack. Sugar-based materials can undergo oxidation using strong oxidizing agents such as potassium permanganate, potassium dichromate, and nitric acid, to result in aldehyde and carboxylic acid compounds. However, this process can also cause significant structural damage of the sugars [24,25]. Persulfates are inexpensive and relatively mild oxidizing agents, which can break the glycosidic bonds in the starch molecular structures [26], leading to oxidation of the hydroxyl groups at positions 2 and 3 to aldehydes [18]. Furthermore, under heating conditions, persulfates can easily undergo hydrolysis in aqueous solutions to produce hydrogen peroxide and persulfate ions. They can also degrade the amorphous regions of lignin, hemicellulose, and cellulose, thereby facilitating the involvement of lignin macromolecular chains in many reactions. Compared to other oxidizing agents, persulfates offer greater advantages in lignin-based adhesives [27]. Therefore, in this study, ammonium persulfate (APS) was chosen as the oxidizing agent to oxidize the active hydroxyl groups in starch molecules, aiming to obtain biomass aldehydes; The aldehyde groups can react with the active hydrogen atoms on the phenolic rings of lignin molecules to form lignin-based adhesives with excellent water resistance. Therefore, FT-IR and XPS techniques are employed to confirm the formation of aldehyde groups in the oxidized starch products so that to ensure the liability for potential reactions between the oxidized starch and lignin; Finally, this study also investigates the effects of oxidation time, oxidizing agent dosage, and the starch-to-lignin mass ratio on the adhesive bonding performance of OSTL.

 doi:10.20944/preprints202505.0760.v1

2. Materials and Method

2.1. Materials

Poplar veneer with a moisture content of 8%–10% was sourced from the local wood market. Sodium lignosulfonate was provided by Hefei Gansheng Biotechnology Co., LTD., China. Soluble starch was purchased from Shanghai Macklin Biochemical Co., LTD., China. Ammonium persulfate (APS) was supplied from Tianjin Kemi Chemical Reagent Co., LTD., China. Potassium bromide (KBr) was provided from Shanghai Aladdin Biochemical Technology Co., LTD., China. Distilled water was prepared in the laboratory.

2.2. Preparation of Biodegradable Aldehyde via Oxidation of Starch

At a temperature of 60°C, a certain mass ratio of starch was added into a three-neck flask equipped with a mechanical stirrer to prepare a 50 wt% aqueous solution of starch. After the starch was fully and evenly homogenized, a certain amount of ammonium persulfate ((NH4)2S2O8) as oxidizing agent was charged and stirred for a certain period of time. After the reaction is complete, filter a portion was exposed to freeze-drying to obtain the oxidized starch (OST) in powder form, while storing the remaining OST liquid in the refrigerator for subsequent analysis and use.

2.3. Preparation of Oxidized Starch-Lignin (OSTL) Adhesive

A certain amount of lignin was added to the OST and stirred thoroughly to ensure that the solid content of the OSTL adhesive reached 50%. Then, the temperature of the water bath was raised to 90°C and the reaction continued for 1 hour. The reaction mixture was then cooled to room temperature to obtain the OSTL adhesive. In order to investigate the effect of other reaction variables, different oxidation times (0 h, 3 h, 6 h, 9 h, 12 h) were employed. Furthermore, different amounts of the oxidizing agent (9%, 11%, 13%, 15%, and 17% based on the starch mass) were made the variable while keeping a reaction time of 6 hours at 60°C constant parameters to check the effect on the properties of the resulting OSTL adhesive. In addition, different mass ratios of the oxidized starch to lignin were set at 0.4, 0.6, 0.8, 1.0, and 1.2, to explore the effect on the properties of the adhesive.

2.4. Fourier Transform Infrared (FT-IR) Spectroscopy Investigation

The uncured adhesive sample was dried in a freez-dryer while the cured adhesive sample was dried in an oven at 200°C, then each was mixed uniformly with potassium bromide in 1:200 ratio and pressed into pellets. Then, the background interference was removed during scanning the samples using Nicolet 670 spectrometer over the wavenumber range of 4000 cm-1 to 400 cm-1 for a total of 32 scans with a resolution of 4 cm-1.

2.5. Proton Nuclear Magnetic Resonance (1H-NMR) Investigation

The freeze-dried adhesive was dissolved in deuterium oxide (D2O). The proton nuclear magnetic resonance (1H-NMR) spectrum was collected for the sample using AVANCE NEO 500 spectrometer (Bruker Corporation, Switzerland). The standard "zg3D" Bruker pulse sequence was applied for recording while a frequency of 500 MHz was operated with 65536 data points collected over 16 scans. The relaxation delay was set to 3.28 seconds, and the chemical shifts were referenced relative to the deuterated solvent (D2O).

2.6. X-Ray Photoelectron Spectroscopy (XPS) Investigation

Using Al Kα excitation as a radiation source with an excitation energy of 1486.6 eV, the adhesive samples were examined before and after curing using the Thermo Scientific K-alpha XPS spectrometer. Charge correction was applied with respect to the binding energy of C 1s at 284.8 eV.

2.7. Evaluation of Three-Layer Plywood Samples

 doi:10.20944/preprints202505.0760.v1

Three-layer plywood was prepared using poplar veneers with dimensions of 180 mm × 110 mm × 2 mm for each layer. The adhesive was applied on the surface of the specimen with a glue amount of 300 g/m², and the pressing time was 10–15 min.. After which, the plywood samples were pressed using a press machine that was purchased from Kunshan Rugong Precision Instrument Co., LTD, China, at different hot-pressing temperatures: 160°C, 170°C, 180°C, 190°C, and 200°C, with a unit pressure of 1 MPa, and a pressing time of 5 minutes. The obtained plywood samples were allowed to acclimate at room temperature for at least 24 hours. Following this, the plywood samples were cut into standard test specimens as shown in Figure 1 according to the testing requirements specified in the national standard GB/T 17657-2022 for plywood bonding strength. According to the national standard GB/T 17657-2022, the testing for dry shear strength, 24-hours cold water soaking strength (20±3°C), 3-hours hot water soaking strength (63±3°C) was conducted to assess the plywood's resistance to boiling water. Additional 3 hours of testing soaking strength The values for each set of bonding strength evaluation are the averages of 6 measurements.

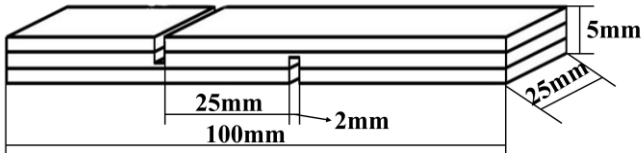

Figure 1. A schematic diagram revealing the dimensions used for three-ply plywood preparation for shear strength testing.

2.8. Estimation of the Hydrolysis Residue Weight of the Cured Adhesive

After curing of the adhesive samples in a high-temperature oven at 200±3°C, the samples were ground into 100-mesh powder. The adhesive powder was wrapped using a filter paper and immersed in water at 63±3°C. After 3 hours of hydrolysis, it was dried to constant weight in an oven at 120±2°C. The residual ratio of the adhesive based on the mass ratio before and after hydrolysis was calculated according to the following formula:

$$\text{residue ratio} = \frac{m_2}{m_1} \times 100\%$$

where m_1: mass of cured adhesive before immersion ; m_2: mass of the cured adhesive after immersion.

2.9. Antifungal Performance of the Adhesive

The antifungal activity was evaluated following a method described in the literature[112], where the starch sample (raw, OST , and OSTL) was prepared into 50% solution, and each solution was placed in a petri dish at room temperature and 90% humidity. The samples were observed at different time intervals for any sign of fungal growth or degradation.

2.10. Differential Scanning Calorimetry (DSC) Investigation

Test the adhesive samples were tested using NETZSCH DSC204F1 differential scanning calorimeter under a flowing nitrogen gas from 35°C to 250°C at a heating increment rate of 10°C/min.

2.11. Dynamic Mechanical Analysis (DMA) Investigation

poplar veneer specimens were cut with the grain into small pieces measuring 50 mm × 10 mm × 2 mm each. The adhesive was applied evenly to one piece of wood, with a glue amount of 300 g/m². Then, another piece of wood was placed on the top and the specimens were allowed to rest for 15 minutes. The specimens were tested in a three-point bending mode at a heating rate of 5 K/min, from 35°C to 300°C, with a frequency of 20 Hz, and dynamic force of 2 N using DMA-242 analyzer, NETZSCH, Germany, and the results were recorded and processed using Proteus analysis software.

 doi:10.20944/preprints202505.0760.v1

2.12. Thermogravimetric Analysis (TGA)

The cured OSTL adhesive was subjected to thermogravimetric analysis (TGA) using Netzsch STA 2500 , TA Instruments, Germany. A temperature range from 30°C to 800 °C was scanned at a heating rate of 10 K/min.

3. Results and Discussion

3.1. Structural Analysis of OST

The FT-IR spectrum of starch (ST) shows some characteristic features: a broad and intense absorption band around 3400–3500 cm-1 attributed to O-H stretching vibrations, peaks at 2928 cm-1 and 2850 cm-1 corresponding to -CH2- stretching vibrations, a peak at 1639 cm-1 indicating bending vibrations of hydroxyl groups in the starch molecular structure, and bands between 945–1209 cm-1 representing stretching vibrations of C-C, C-O, and C-O-C bonds[28]. On the other hand, the FT-IR spectrum of oxidized starch (OST) reveals emergence of a new peak at 1725 cm-1 attributed to the stretching vibration of (C=O) groups resulting from the oxidation. This indicates the formation of aldehyde or carboxyl groups after oxidation. Additionally, the signals between 945–1209 cm-1 mitigated, suggesting molecular chain fragmentation and depolymerization of starch molecules during the oxidation process.

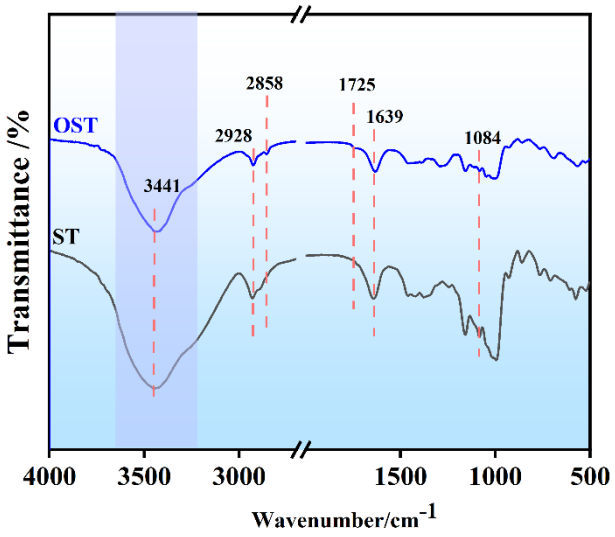

Figure 2. FT-IR spectra of starch (ST) and oxidized starch (OST).

To elucidate the products of oxidized starch in this study, 1H-NMR spectroscopic analysis was conducted on ST and OST. As shown in Figure 3, the 1H-NMR spectra of starch before and after oxidation reveal some structural differences. For OST, signals indicating aldehyde (CHO) groups appeared at 8.00 – 8.50 ppm, indicating successful oxidation of ST. According to previous studies [29], the C2-C3 bond of glucose units in the starch undergoes cleavage, resulting in formation of two aldehyde units. However, the aldehyde signals in Figure 3-2 are relatively weak. Some studies attributed that to an associated following formation of hemiacetal structures [30].

 doi:10.20944/preprints202505.0760.v1

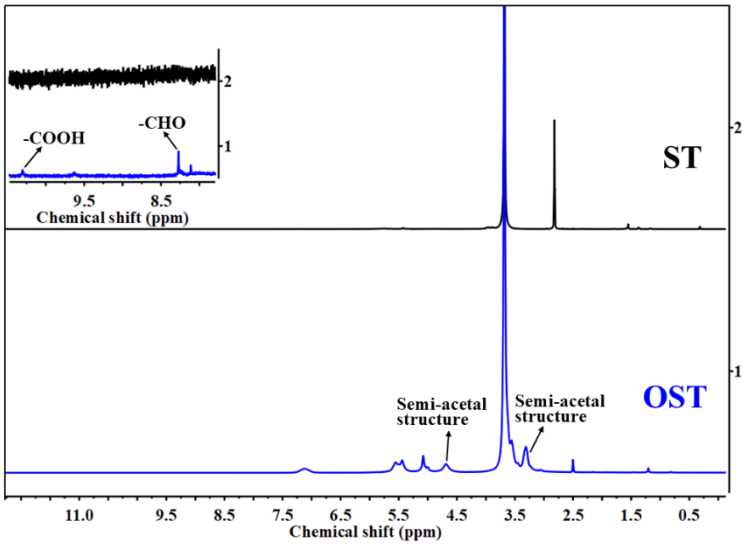

Figure 3. 1H-NMR spectra of starch (ST) and oxidized starch (OST).

It was thus suggested that in this equilibrium system, there were aldehyde hydrates and hemiacetal groups, while free aldehydes were absent [29]. Furthermore, the high sensitivity of 1H-NMR spectroscopy enabled the detection of a relatively weak signal at 10.50 ppm which presents an evidence for carboxyl groups (COOH) formation. This also indicates that some hydroxyl groups in the starch structure encountered excessive oxidation to form carboxyl groups.

To further validate the previous speculations, X-ray photoelectrons spectroscopic (XPS) analysis was conducted on ST and OST as shown in Figure 4. Figure 4 (c) displays the C 1s spectrum of ST, showing signals at 286.52 eV, attributed to C-O bonds, and at 288.12 eV attributed to C-O-C bonds. In comparison, the C 1s spectrum of OST reveals a signal peak at 287.76 eV, attributed to aldehyde groups and another peak at 289.00 eV, referring to carboxyl groups. The elemental composition analysis of C 1s was collected in Tables 1 and 2 for ST and OST, respectively, where it can be realized that the OST has a higher content of aldehyde groups, and only a small amount of starch may have been over-oxidized to form carboxylic acids. This is consistent with the obtained data from FT-IR and 1H-NMR. In summary, based on the FT-IR, 1H-NMR, and XPS spectroscopic analyses, a tentative structure of oxidized starch is depicted in Figure 5.

 doi:10.20944/preprints202505.0760.v1

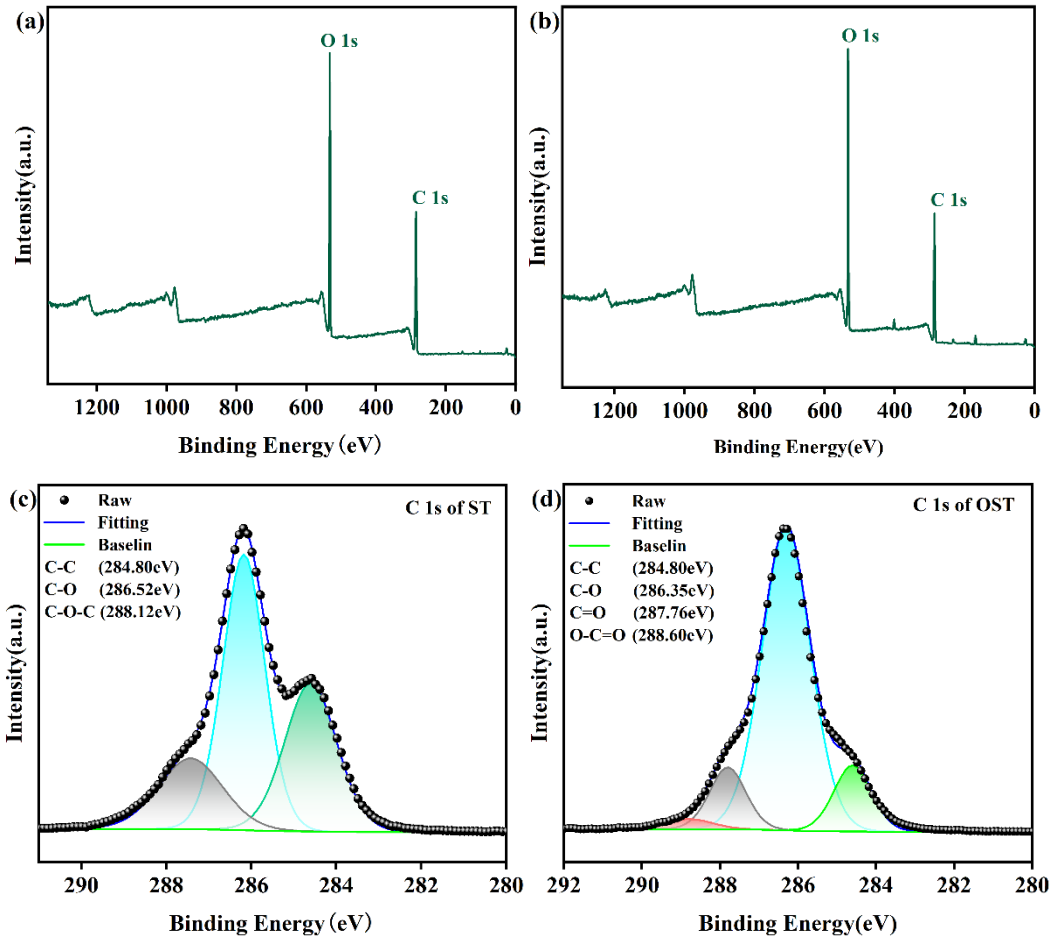

Figure 4. XPS spectra of ST and OST. (a) XPS full measurement spectra of ST; (b) XPS full measurement spectra of OST; (c) High-resolution C 1s spectrum of ST; (d) High-resolution C 1s spectrum of OST.

Table 1. Elemental composition of C 1s in ST.

Name	peak	FWHM (eV)	Area(P) CPS. eV	Atomic (%)
C-C	284.80	1.21	46384.29	35.70
C-O	286.52	1.51	69450.80	53.45
C-O-C	288.12	1.84	14109.65	10.86

Table 2. Elemental composition of C 1s in OST.

Name	peak	FWHM (eV)	Area(P) CPS. eV	Atomic (%)
C-C	284.80	1.34	23135.67	16.07
C-O	286.35	1.38	98516.11	68.44
C=O	287.76	1.21	16834.70	11.70
O-C=O	288.60	1.48	5449.34	3.79

 doi:10.20944/preprints202505.0760.v1

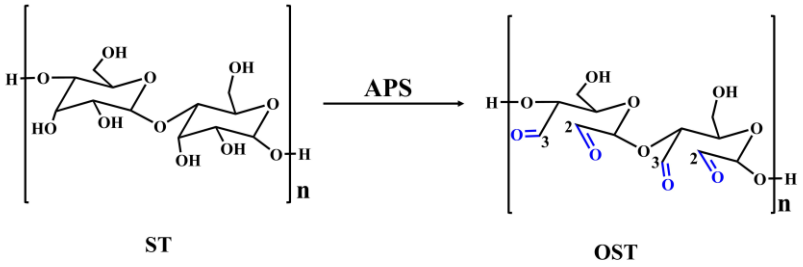

Figure 5. The process of oxidizing ST to generate OST using APS as oxidizing agent.

3.2. Structural Characterization of the OSTL Adhesive

The FT-IR spectra of oxidized starch (OST), lignin (L), and the adhesive OSTL, before and after curing, are displayed in Figure 6. The peak at 1725 cm-1, attributed to carbonyl (C=O) groups, is present in OST, OSTL-1, and OSTL-2. No new peaks could be recognized in the adhesive before and after curing whereas some slight shifts and a little change in peaks intensities prove the curing was not other than some bonds breakage and re-formation of another.

Therefore, to further investigate that, X-ray photoelectron spectroscopy (XPS) analysis was accomplished on the adhesive samples before and after curing (Figure 7). From Figure 7, it is evident that there was no new functional groups formed in the adhesive before and after curing in the sense of chemical environments. However, XPS can quantitatively analyze the elemental content as illustrated in Tables 3 and 4. The change in the O 1s elemental content of the OSTL adhesive reveals that the content attributed to aldehyde groups at 531.30 eV decreased from 6.05% before curing to 0.14% after curing. This reduction is attributed to the consumption of aldehyde groups in reactions during curing, leading to a significant decrease in their content. Additionally, from Tables 3 and 4, it can be observed that the content of O-C=O increased from 0.04% before curing to 0.24% after curing. This signifies that the present carboxyl groups formed due to over-oxidation can undergo esterification reactions with hydroxyl groups in lignin during curing, leading to an increase in the O-C=O content. Therefore, the reaction between oxidized starch and lignin involves an addition reaction between aldehyde groups and active sites in lignin, and the esterification of carboxyl groups derived from oxidized starch with hydroxyl groups on lignin.This can also extend to acetal or hemiacetal formation. These processes collectively promote the degree of crosslinking in the OSTL adhesive, leading to the formation of a robust crosslinked network structure, thereby enhancing the bond strength of the adhesive.

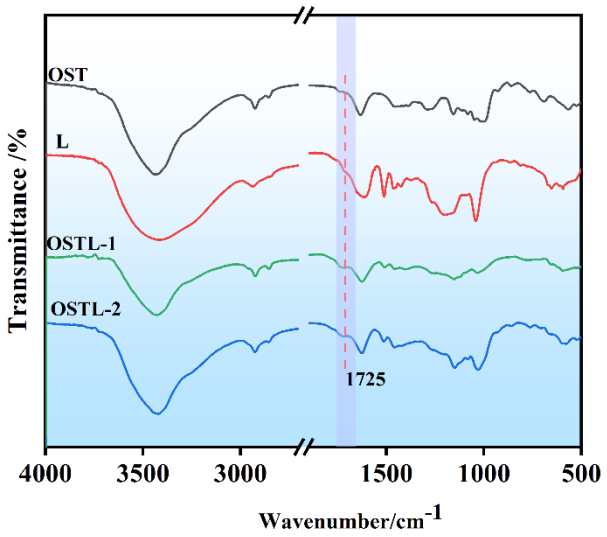

 doi:10.20944/preprints202505.0760.v1

Figure 6. (a) FT-IR spectra of OST, lignin (L), OSTL-1 (uncured resin adhesive), and OSTL-2 (cured resin adhesive).

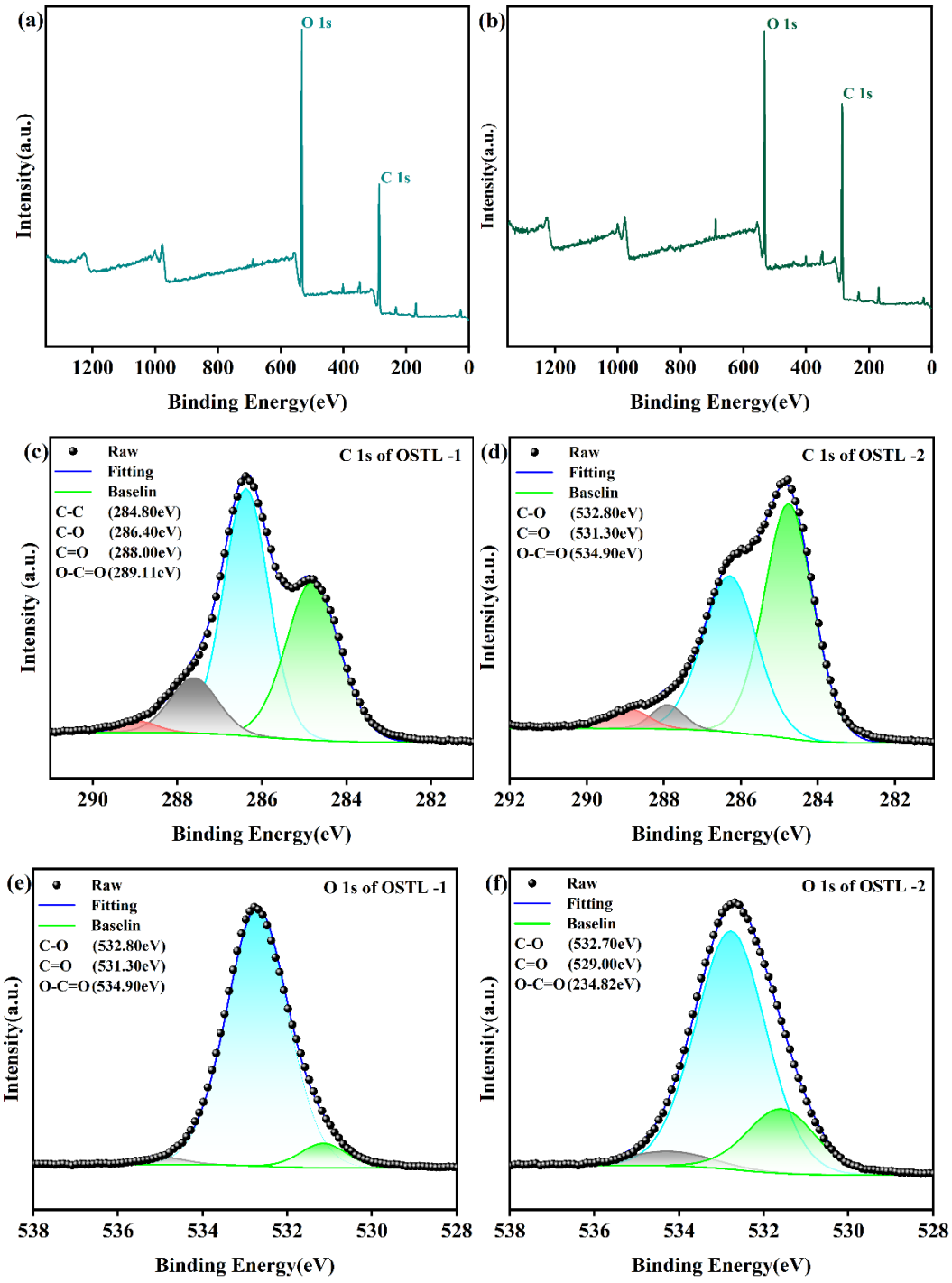

Figure 7. XPS spectra of OSTL-1 and OSTL-2. (a) XPS full measurement spectra of OSTL-1; (b) XPS full measurement spectra of OSTL-2; (c) High-resolution C 1s spectrum of OSTL-1; (d) High-resolution C 1s spectrum of OSTL-2; (e) High-resolution O 1s spectrum of OSTL-1; and (f) High-resolution O 1s spectrum of OSTL-2.

Table 3. Elemental composition of O 1s in OSTL-1.

Name	peak	FWHM (eV)	Area(P) CPS. eV	Atomic (%)
C-O	532.80	1.85	212974.74	93.92
C=O	531.30	1.29	13710.86	6.05
O-C=O	534.90	1.30	86.48	0.04

 doi:10.20944/preprints202505.0760.v1

Table 4. Elemental composition of O 1s in OSTL-2.

Name	peak	FWHM (eV)	Area(P) CPS. eV	Atomic (%)
C-O	532.70	2.48	158164.89	99.62
C=O	529.00	0.54	225.13	0.14
O-C=O	534.82	0.54	373.98	0.24

3.3. Evaluation of the Antifungal Performance of Adhesives

Starch, a polysaccharide composed of anhydroglucose units, ranks as the second most abundant carbohydrate in plants. It serves as a crucial carbon source for microbial growth and reproduction. However, starch is highly susceptible to fungal infection [31,32], which limits its industrial applications significantly. As can be shown in Figure 8, the antimicrobial properties of various liquid samples were exmined over one month, under conditions of room temperature and 90% relative humidity. It is noteworthy that mold growth begins to appear around the 13th day in starch-based materials, and as time progresses, the mold spreads further, gradually covering the entire base liquid of the culture dish. In contrast, oxidized starch and the samples cross-linked with lignin did not show any mold erosion, indicating that oxidized starch (OST) indeed acquired certain antifungal properties [33,34]. Meanwhile, lignin possesses natural antimicrobial properties [35], enabling the prepared OSTL adhesive to largely resist fungal corrosion.

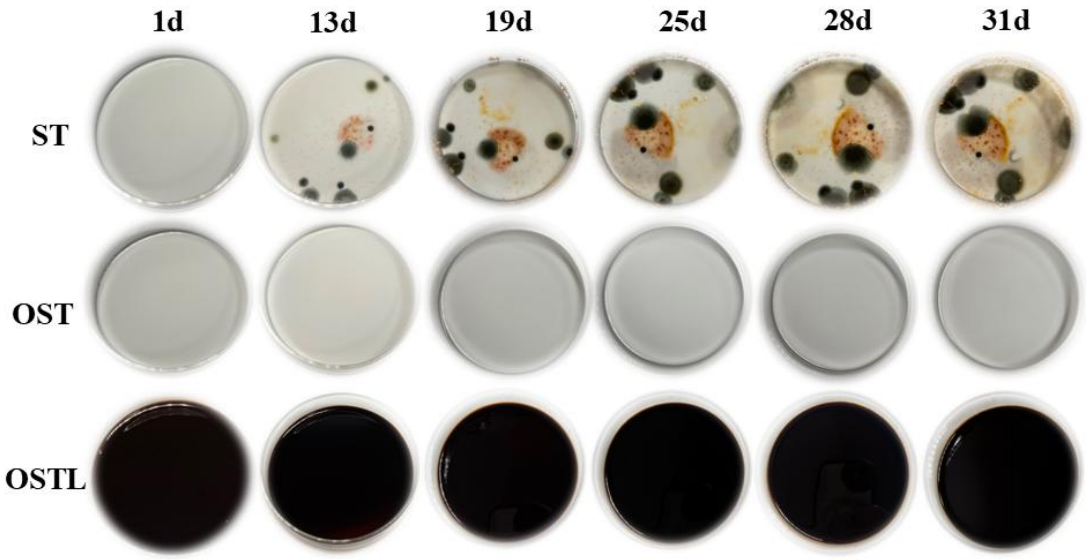

Figure 8. Mold resistance testing of starch (ST), oxidized starch (OST) and OSTL adhesive in liquid form.

3.4. The Effect of Different Oxidation Times on the Performance of OSTL Adhesives

Figure 9(a) illustrates the effect of different oxidation times on the adhesive performance of OSTL. It is obvious from the figure that up to 6 hours of oxidation time, both dry and wet shear strengths of the adhesive increase with prolongation of the oxidation times. For an oxidation time of 3 hours, the shear strength of the OSTL adhesive-prepared plywood already meets the standards for Class II plywood specified in GB/T17657-2022. However, with further extension of oxidation time, the hot water (63±3℃) shear strength of the adhesive decreases. This may present a proof that with prolonged time, oxidized starch readily undergoes aldol condensation with hydroxyl groups in the system, forming hemiacetals, thereby reducing the aldehyde content in the system. This may also be attributed to the over-oxidation, which can act in different ways to weaken the tendency of oxidized starch for further reaction with lignin.

 doi:10.20944/preprints202505.0760.v1

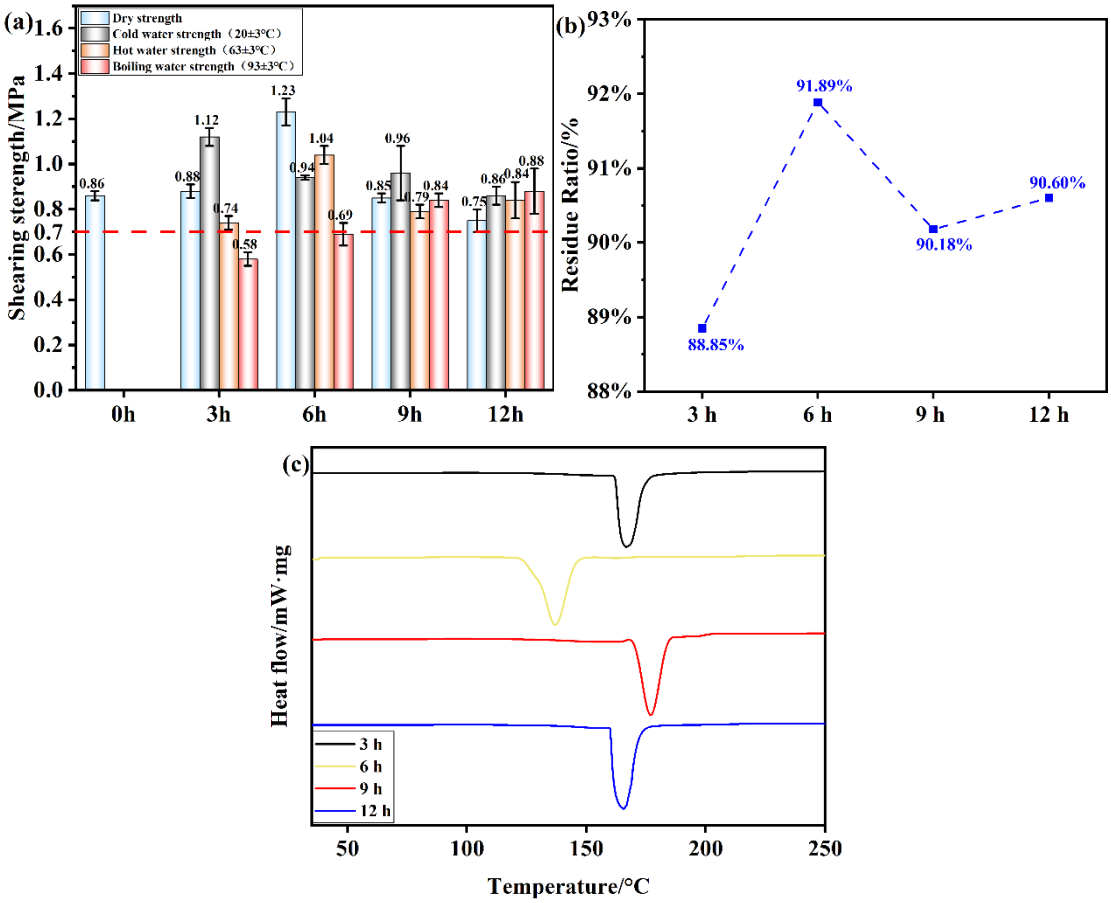

Figure 9. (a) Shear strength of plywood prepared using OSTL adhesives prepared under different oxidation times of OST as precursor ; (b) Hydrolysis residual rate of OSTL adhesive under different oxidation times of OST as precursor; (c) DSC traces of OSTL adhesives prepared under different oxidation times of OST as precursor.

Additionally, to further verify the water resistance of the adhesive, this study also extended to testing the residual curing hydrolysis rate of the adhesive (Figure 9(b).At an oxidation time of 3 hours, the hydrolysis residual rate reached 88.85%. Increasing the oxidation time further to 6 hours results in the highest residual rate of 91.89% for the adhesive. However, beyond 6 hours of oxidation, most of the aldehyde groups in the oxidized starch was converted to the hemiacetals forms. This results in insufficient aldehyde groups available for reaction with lignin, leading to in-sufficient cross-linking reactions and an unstable cross-linked network structure in the adhesive. Consequently, the adhesive becomes more susceptible to attack by water molecules, reducing its water resistance. This correlates well with the adhesive's bonding performance results.

The bond strength and water resistance of adhesive are important criteria for evaluating the adhesive bonding performance. However, overall performance of an adhesive can be not be solely decided from these parameters alone. Therefore, a thermal investigation was performed using differential scanning calorimetry, which is thought to reflect important information about the curing performance of the adhesives along with the thermal transition temperatures and heat flow relationships within the adhesive, assessing the absorption or release of energy as a function of temperature [36]. This included the OSTL adhesives prepared under different oxidation times of the OST as precursor, as shown in Figure 9(c). It can be observed that for an oxidation time of 6 hours, the adhesive sample exhibits a distinct exothermic peak below 150°C, whereas the exothermic peaks for the adhesives formulated with other oxidation time conditions occurred at temperatures higher than 150°C (Table 5). This indicates that maximum reactivity could be attained for 6 hours as oxidation time of starch, and this assumption was supported by the adhesive acquired a lower apparent activation energy for curing. This also reflects that within a certain range of oxidation time, a highest level of aldehyde groups content can be achieved, leading to a higher activity and lower

 doi:10.20944/preprints202505.0760.v1

heat required for curing reactions. This opyimal level should also contribute to a more stable performance. Based on this, an oxidation time of 6 hours is considered appropriate.

Table 5. Curing characteristics of OSTL adhesives formulated from OST prepared under different oxidation times.

Time/h	Starting temperature/℃	Maximum exothermic peak/℃	Termination temperature/℃	Enthalpy/ (J.g^{-1})
3	162.0	166.8	174.2	951.7
6	128.1	137.0	145.1	951.4
9	169.7	176.9	184.5	1156.0
12	159.4	165.4	172.2	1024.0

3.5. Effect of Oxidizing Agent Dose on the Performance of OSTL Adhesives

The oxidant is an important reactant used in the modification of starch, directly affecting the degree of starch oxidation. The effect of oxidant addition amount on the shear strength of plywood prepared using OSTL adhesive is shown in Figure 10(a), from which it can be observed that with an increasing amount of APS as oxidant, the wet shear strength of plywood prepared using OSTL adhesive gradually increases. With an oxidant amount of 13%, the plywood's hot water (63±3℃) shear strength reached 1.04 MPa, meeting the standards for Class II plywood specified in Chinese GB/T17657-2022. As the oxidant APS gradually increased, although the wet shear strength of the plywood also increased, there was a drop in shear strength. This is simply justified by over-oxidation took place on the starch due to an excess of APS, leading to insufficient level of aldehyde groups to undergo good reaction with the lignin, whereas the plenty of formed COOH could cause some damage to the wood itself, resulting in reduced toughness and mechanical performance of the plywood.

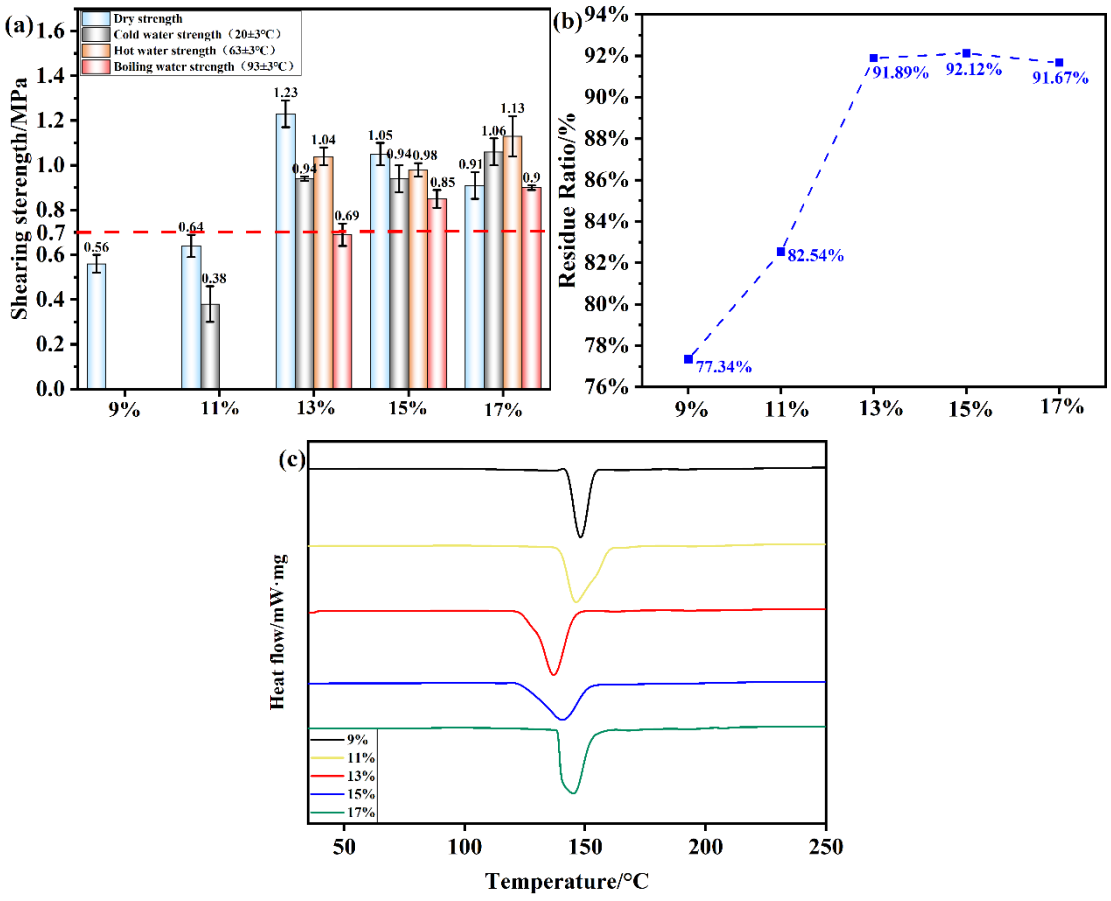

 doi:10.20944/preprints202505.0760.v1

Figure 10. (a) Shear strength of plywood prepared using OSTL adhesives formulated with OST prepared using different oxidant additions; (b) Hydrolysis residual rate of OSTL adhesives formulated with OST prepared with different oxidant additions; (c) DSC curve of OSTL adhesives formulated with OST prepared using different oxidant additions.

This study also investigated the residual curing hydrolysis rate of OSTL adhesive under different oxidant addition amounts as shown in Figure 10(b). Similarly, with an increase in the oxidant level, the residual curing hydrolysis rate significantly increased. When the adhesive reached a maximum residual rate of 92.12% at an oxidant addition of 15%, it subsequently decreased to 91.67% when the oxidant level exceeded to 17%. This suggests that the adhesive's water resistance does not directly correlate with increasing the oxidant amount for the range 13-17%.

Figure 10(c) reveals the conducted DSC study for the samples formulated with OST obtained under varying oxidant addition amounts while keeping other conditions constant. It can be seen that the temperatures of obtained exothermic peaks during curing of the adhesive vary with the different oxidant addition amounts. This explains that the oxidant indeed plays an important role in influencing the curing reaction of the adhesive. Table 6 reveals the curing temperatures and corresponding reaction enthalpy of the adhesive under different oxidant addition amounts. At 13% and 15% oxidant levels, the adhesive exhibited lower initial curing temperatures, but the peak curing temperature at 13% was lower compared to that at 15%, while the curing enthalpy at 13% was higher than that at 15%. Hence an oxidant addition of 13% may be the most appropriate for formulations with lignin. Furthermore, from an economic perspective, adding a small amount of oxidant can achieve excellent bonding performance for the adhesive. Therefore, in this study, 13% was selected as the most suitable oxidant amount.

Table 6. Curing characteristics of OSTL adhesives formulated with OST prepared using different oxidant additions.

Additions /%	Starting temperature/℃	Maximum exothermic peak/℃	Termination temperature/℃	Enthalpy/ (J.g^{-1})
9	142.8	148.1	153.5	666
11	144.0	154.8	162.1	997.4
13	128.1	137.0	145.1	951.4
15	125.5	141.1	150.1	814.2
17	126.3	140.5	149.8	779.8

3.6. The Impact of Different Mass Ratios of Starch to Lignin on the Performance of OSTL Adhesives

In order to further explore the influence of other factors on the bonding performance of OSTL adhesives, this study also investigated the performance variation of the adhesives prepared with different starch-to-lignin mass ratios. As shown in Figure 11(a), it can be observed that as the mass ratio of starch to lignin increases from 0.4 to 0.8, the dry shear strength of plywood prepared using OSTL adhesive also increases from 0.46 MPa to at least 1.23 MPa, achieving almost 3 times increase. This clearly demonstrates that increasing the amount of starch, under the same oxidant addition, likely provides more active aldehyde groups. This can effectively improve the bonding strength of lignin-based adhesives. It can be noticed that at a mass ratio of 0.8, the specimen's hot water shear strength reached 1.04 MPa, showing a significant improvement. However, with the increase in mass ratio, both the dry shear strength and wet shear strength of the specimens decreased. This could be because all active reaction sites on lignin became already involved in reactions. Increasing the starch content further may not effectively participate in cross-linking reactions with lignin. Additionally, excessive starch amounts may contain unoxidized hydroxyl groups, which are so hydrophilic and can reduce the water resistance of the adhesive. From Figure 11(b), the residual hydrolysis rate of the

 doi:10.20944/preprints202505.0760.v1

adhesive prepared under different mass ratios confirms this assumption: as the mass ratio increases, the adhesive's residual rate initially increases significantly and then decreases.

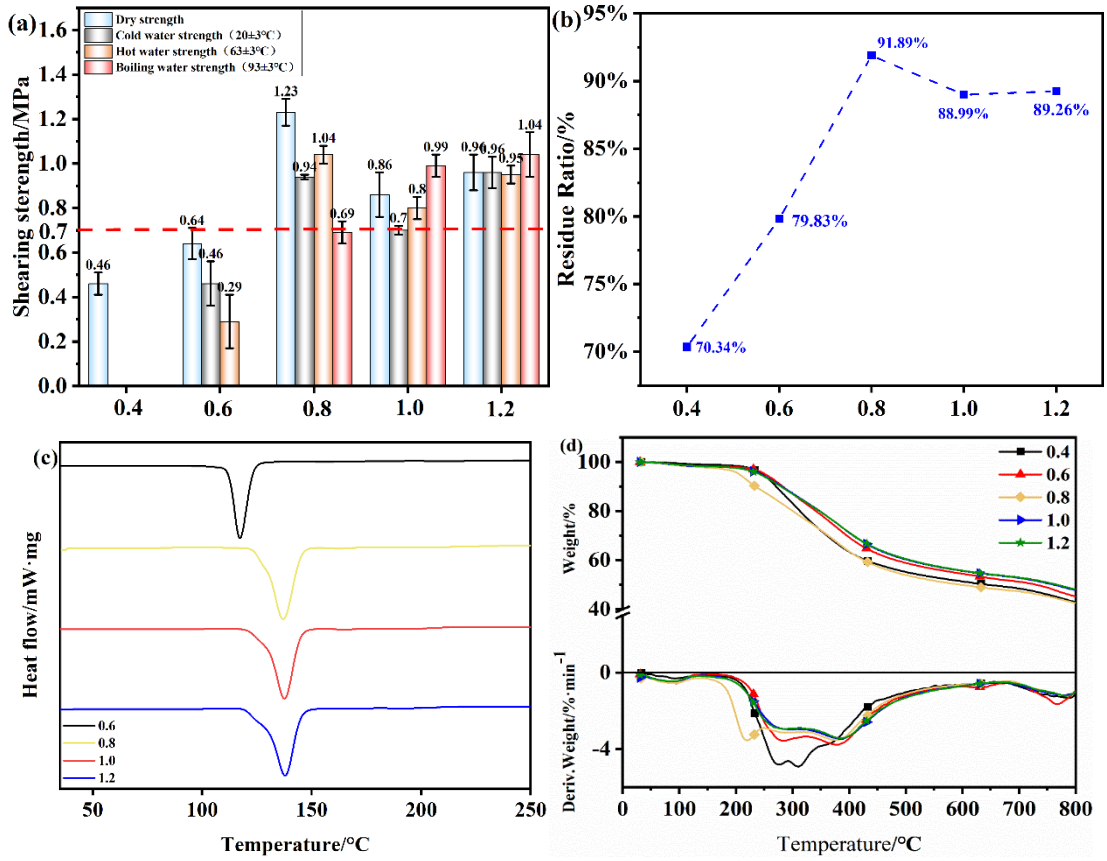

Figure 11. (a) Shear strength of plywood prepared using OSTL adhesives prepared with different starch to lignin mass ratios; (b) Hydrolysis residual rate of OSTL adhesives prepared with different starch to lignin mass ratios; (c) DSC thermograms of OSTL adhesives prepared with different starch to lignin mass ratios; (d) TGA traces of OSTL adhesives prepared with different starch to lignin mass ratios.

Figure 11(c) and (d) depicts the thermal performance of the adhesives prepared under different mass ratios. Figure 11(c) reveals the DSC traces of OSTL adhesives prepared under different mass ratios, complemented by the curing temperature and reaction enthalpy values (Table 7). As the mass ratio increases, the adhesive's initial temperature of 110.5°C was the lowest for the ratio 0.6, indicating un-matured degree of cross-linking and less stable cross-linked network structure within the adhesive. This may correlate with the lower water resistance, consistent with the residual rate results of the adhesive. As the mass ratio continues to increase, especially at a ratio of 0.8, the adhesive exhibits the lowest initial curing temperature and highest enthalpy, indicating the reaction became more favored leading to a deeper degree of curing. Therefore, at a ratio of 0.8, the adhesive may provide better performance, consistent with the results of the adhesive's residual hydrolysis rate.

Figure 11(d) shows the TGA and relevant DTG traces of OSTL adhesives prepared under different mass ratios of starch to lignin. As seen from the figure, with the increase in temperature, all adhesive samples exhibited the same weight loss pattern. In the temperature range of 30–230°C (Region I), a relatively low weight loss of about 10% is observed, which is likely due to the evaporation of small molecular substances and adsorbed/entrapped water [37]. In the temperature range of 230–500°C (Region II), the primary phase of mass loss occurs, likely due to the breakdown of the adhesive's cross-linked network and intensive degradation of the polymer chains within the molecular structure [38]. As the mass ratio increases, the initial decomposition temperature gradually increases. For example, the initial decomposition temperature is the lowest at a ratio of 0.4 and highest at a ratio of 1.2. This indicates that as the mass ratio increases, the higher aldehyde content effectively

 doi:10.20944/preprints202505.0760.v1

enhances the degree of cross-linking between the chains, rendering the adhesive more resistant to thermal degradation.

Finally, based on the comprehensive analysis of adhesive bonding strength, residual hydrolysis rate, and thermal performance, it can be concluded that the adhesive exhibits optimal performance at a starch-to-lignin mass ratio of 0.8.

Table 7. Curing characteristics of OSTL adhesives prepared with different starch to lignin mass ratios.

Starch	Starting temperature/℃	Maximum exothermic peak/℃	Termination temperature/℃	Enthalpy/ (J.g^{-1})
0.6	110.5	127.5	137.9	689.2
0.8	128.1	137.0	145.1	988.2
1.0	128.3	137.8	144.9	970.2
1.2	128.7	138.1	145.1	978.0

3.7. Effect of Different Hot-Pressing Temperatures on the Performance of OSTL Adhesives

Figure 12(a) shows the mechanical strength of the plywood bonded with OSTL adhesives prepared under different hot-pressing temperatures. It can be observed that as the hot-pressing temperature increases, both the dry and wet shear strength of the adhesive gradually improves. Combining this with the analysis of the adhesive's water resistance shown in Figure 12(b), it can be realized that the reaction only occurs fully at higher temperatures. This may be because the lignin grade used in this study is industrial lignin, which has a higher degree of condensation then provides fewer active reaction sites. Starch, as a macromolecular polysaccharide, also requires higher temperatures to undergo maximum cross-linking reaction between the two macromolecular reactants.

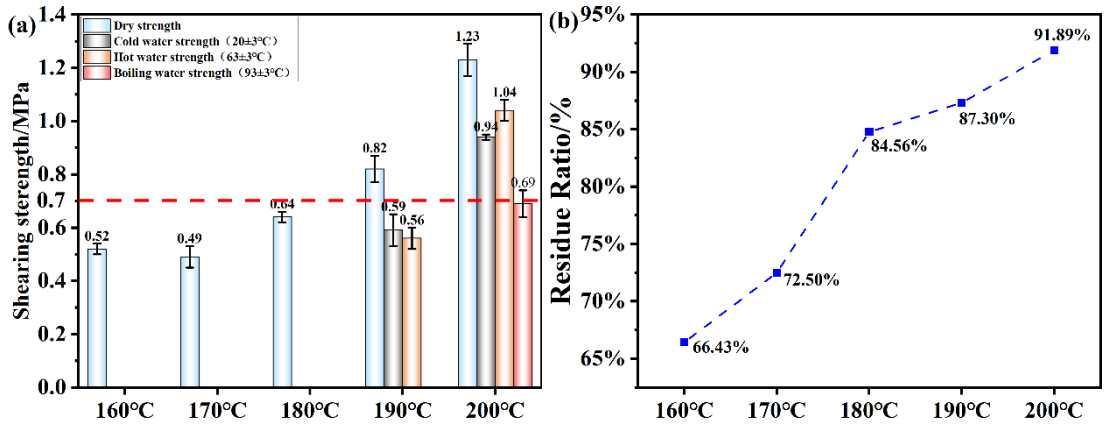

Figure 12. (a) Shear strength of plywood prepared using OSTL adhesives prepared at different hot-pressing temperatures; (b) Hydrolyzed residual rate of OSTL adhesives prepared at different hot-pressing temperature.

4. Conclusion

Oxidation of starch represents a good approach for obtaining biomass aldehyde compounds, which can then be reacted with lignin to prepare environmentally friendly biomass adhesives. The oxidation process should be carefully undertaken under good control to ensure minimal level of over-oxidation, which is associated by carboxyl groups formation on the expense of the more active aldehyde groups. The aldehyde groups undergo addition reactions with the active sites on lignin, while the carboxyl groups formed due to over-oxidation undergo esterification with the hydroxyl groups in lignin. This process should be balanced in order to ensure robust cross-linked network structure by the adhesive curing and elevated bonding performance. The mechanical performance of prepared plywood and residual hydrolysis rate testing explained that under the conditions of 6 hours

 doi:10.20944/preprints202505.0760.v1

as oxidation time, oxidant addition of 13% based on the starch mass, and a starch-to-lignin mass ratio of 0.8, with a hot-pressing temperature of 200°C, can ensure OSTL adhesive bearing excellent bonding performance. The plywood prepared using adhesive prepared under optimized conditions can achieve a dry shear strength of 1.23 MPa, cold water (24 hours) shear strength of 0.94 MPa, and hot water (63±3°C, 3 hours) shear strength of 1.04 MPa, to adhere perfectly to the Chinese standard GB/T17657-2022 for Grade II plywood, at this time the boiling water of the plywood reaches 0.69 MPa. This was also confirmed from thermal analysis conducted using DSC and TGA. Investigation that were in complete accordance with other data.

Author Contributios: Chengyuan Liu and Huali Lin: Writing- review & editing, Writing-original draft, Methodology. Shichao Zhang and Longxu Wu: Methodology, Data curation, Supervision, Formal analysis. Hongyan Wang and Xinyi Chen: Writing- review & editing, Validation, Supervision. Antonios N. Papadopoulos: Writing- review & editing, Validation, Supervision, Conceptualization. Antonio Pizzi and Xiaojian Zhou: Writing- review & editing, Methodology, Conceptualization. Hisham Essawy: Writing- review & editing, Methodology, Data curation. Ming Cao: Writing-review & editing, Resources, Project administration.

Acknowledgments: This study received financial support by Yunnan Provincial High-level Talents Training Support Plan Youth Top Talent Project (Grant No. YNWR-QNBJ-2020-144), the National Natural Science Foundation of China (Grant No. 31800483), and the Agriculture Joint Research Program of Yunnan Province (Grant No. 2017FG001 (-079)). Additionally, this study was supported by the International Joint Research Center for Biomass Materials (Southwest Forestry University) (Grant No.2023-GH02), the 111 Project (Grant No. D21027), Foreign Expert Workstation (Grant No. 202305AF150006) and the Major Science and Technology Project of Yunnan Province (202402AE090027).

References

1. Li R. J., Gutierrez J., Chung Y. L., et al. A Lignin-Epoxy Resin Derived from Biomass as an Alternative to Formaldehyde-Based Wood Adhesives. *J. Green Chemistry, The Royal Society of Chemistry*. 2018, 20(7): 1459–1466.
2. Shi X., Gao S., Jin C., et al. A Facile Strategy to Fabricate a Lignin-Based Thermoset Alternative to Formaldehyde-Based Wood Adhesives. *J. Green Chemistry, The Royal Society of Chemistry*. 2023, 25(15): 5907–5915.
3. Balk M, Sofia P, Neffe A T, et al. Lignin, the lignification process, and advanced, lignin-based materials. *J. International journal of molecular sciences*. 2023, 24(14): 11668.
4. Rath S, Pradhan D, Du H, et al. Transforming lignin into value-added products: Perspectives on lignin chemistry, lignin-based biocomposites, and pathways for augmenting ligninolytic enzyme production. *J. Advanced Composites and Hybrid Materials*. 2024, 7(1): 27.
5. Sarkar S., Adhikari B. Lignin-Modified Phenolic Resin: Synthesis Optimization, Adhesive Strength, and Thermal Stability. *J. Journal of Adhesion Science and Technology*. 2000, 14(9): 1179–1193.
6. Nonaka Y., Tomita B., Hatano Y. Synthesis of Lignin /Epoxy Resins in Aqueous Systems and Their Properties. *J. hfsg*. 1997, 51(2): 183–187.
7. N.-E. El Mansouri, Pizzi A., Salvado J. Lignin-Based Polycondensation Resins for Wood Adhesives. *J. Journal of Applied Polymer Science*. 2010, 103(3): 1690–1699.
8. Mansouri H. R., Pizzi A. Urea–Formaldehyde–Propionaldehyde Physical Gelation Resins for Improved Swelling in Water. *J. Journal of Applied Polymer Science*. 2006, 102(6): 5131–5136.
9. Wu Z., Xi X., Lei H., et al. Soy-Based Adhesive Cross-Linked by Phenol-Formaldehyde-Glutaraldehyde. *J. Polymers.* 2017, 9(12): 169.
10. El-Mansouri N, Pizzi A, Salvadó J. Lignin-based wood panel adhesives without formaldehyde. *J. HOLZ ROH WERKST.* 2007, 65: 65–70.
11. Van Nieuwenhove I., Renders T., Lauwaert J., et al. Biobased Resins Using Lignin and Glyoxal. *J. ACS Sustainable Chemistry & Engineering*. 2020, 8(51): 18789–18809.

 doi:10.20944/preprints202505.0760.v1

12. Hazwan Hussin M., Aziz A. A., Iqbal A., et al. Development and Characterization Novel Bio-Adhesive for Wood Using Kenaf Core (Hibiscus Cannabinus) Lignin and Glyoxal. *J. International Journal of Biological Macromolecules.* 2019, 122: 713–722.
13. Huzyan H. I., Abdul Aziz A., Hussin M. H. Ecofriendly Wood Adhesives from Date Palm Fronds Lignin for Plywood. *J. BioResources*. 2021, 16(2): 4106–4125.
14. Chupin, Lucie, Pizzi, et al. Study of Thermal Durability Properties of Tannin-Lignosulfonate Adhesives. *J. Journal of Thermal Analysis & Calorimetry*. 2015, 119: 1577–1585.
15. Zhang Y., Yuan Z., Mahmood N., et al. Sustainable Bio-Phenol-Hydroxymethylfurfural Resins Using Phenolated de-Polymerized Hydrolysis Lignin and Their Application in Bio-Composites. *J. Industrial Crops and Products.* 2016, 79: 84–90.
16. Dongre P., Driscoll M., Amidon T., et al. Lignin-Furfural Based Adhesives. *J. Energies*. 2015, 8(8): 7897–7914.
17. Fadlallah S., Sinha Roy P., Garnier G., et al. Are Lignin-Derived Monomers and Polymers Truly Sustainable? An in-Depth Green Metrics Calculations Approach. *J. Green Chemistry*. 2021, 23(4): 1495–1535.
18. Diaz-Baca J. A., Fatehi P. Production and Characterization of Starch-Lignin Based Materials: A Review. *J. Biotechnology Advances*. 2024, 70: 108281.
19. Ferreira-Filipe D. A., Paço A., Duarte A. C., et al. Are Biobased Plastics Green Alternatives?—A Critical Review. *J. International Journal of Environmental Research and Public Health*. 2021, 18(15): 7729.
20. Weiss M., Haufe J., Carus M., et al. A Review of the Environmental Impacts of Biobased Materials. *J. Journal of Industrial Ecology*. 2012, 16: S169–S181.
21. Amagliani L., O'Regan J., Kelly A. L., et al. Chemistry, Structure, Functionality and Applications of Rice Starch. *J. Journal of Cereal Science*. 2016, 70: 291–300.
22. Luchese C. L., Benelli P., Spada J. C., et al. Impact of the Starch Source on the Physicochemical Properties and Biodegradability of Different Starch-based Films. *J. Journal of Applied Polymer Science*. 2018, 135(33): 46564.
23. Van Hung P., Maeda T., Morita N. Waxy and High-Amylose Wheat Starches and Flours—Characteristics, Functionality and Application. *J. Trends in Food Science & Technology*. 2006, 17(8): 448–456.
24. Kristiansen K. A., Potthast A., Christensen B. E. Periodate Oxidation of Polysaccharides for Modification of Chemical and Physical Properties. *J. Carbohydrate Research*. 2010, 345(10): 1264–1271.
25. Vanier N. L., El Halal S. L. M., Dias A. R. G., et al. Molecular Structure, Functionality and Applications of Oxidized Starches: A Review. *J Food Chemistry*. 2017, 221: 1546–1559.
26. Apriyanto A., Compart J., Fettke J. A Review of Starch, a Unique Biopolymer – Structure, Metabolism and in Planta Modifications. *J. Plant Science*. 2022, 318: 111223.
27. Zhao Z. Q., Ouyang X. P. Effect of Oxidation on the Structures and Properties of Lignin. *J. Advanced Materials Research*. 2012, 550–553: 1208–1213.
28. Lin Q., Pan J., Lin Q., et al. Microwave Synthesis and Adsorption Performance of a Novel Crosslinked Starch Microsphere. *J. Journal of Hazardous Materials*. 2013, 263: 517–524.
29. Li J., Du M., Din Z. ud, et al. Multi-Scale Structure Characterization of Ozone Oxidized Waxy Rice Starch. *J. Carbohydrate Polymers*. 2023, 307: 120624.
30. Serrero A., Trombotto S., Cassagnau P., et al. Polysaccharide Gels Based on Chitosan and Modified Starch: Structural Characterization and Linear Viscoelastic Behavior. *J. Biomacromolecules*. 2010, 11(6): 1534–1543.
31. Shao J., Li X., Liu T., et al. Multiple Function Hyperbranched Polysiloxane Nanoclusters for Controlling a Cross-Linking Structure to Convert Soy Meal into a Strong, Tough, and Multifunctional Adhesive. *J. ACS Sustainable Chemistry & Engineering*. 2024, 12(10): 3966–3976.
32. Lyu F., Van Der Poel A. F. B., Hendriks W. H., et al. Particle Size Distribution of Hammer-Milled Maize and Soybean Meal, Its Nutrient Composition and in Vitro Digestion Characteristics. *J. Animal Feed Science and Technology*. 2021, 281: 115095.
33. Song S., Gao P., Sun L., et al. Recent Developments in the Medicinal Chemistry of Single Boron Atom-Containing Compounds. *J. Acta Pharmaceutica Sinica B*. 2021, 11(10): 3035–3059.
34. Hajareh Haghighi F., Mercurio M., Cerra S., et al. Surface Modification of TiO 2 Nanoparticles with Organic Molecules and Their Biological Applications. *J. Journal of Materials Chemistry B*. 2023, 11(11): 2334–2366.

 doi:10.20944/preprints202505.0760.v1

35. Nguyen N Y, Luong H V T, Pham D T, et al. Drug-loaded Fe3O4/lignin nanoparticles to treat bacterial infections. *J. International Journal of Biological Macromolecules*. 2025, 289: 138868.
36. Chen S, Shi S Q, Zhou W, et al. Developments in bio-based soy protein adhesives: a review. *J. Macromolecular Materials and Engineering*. 2022, 307(10): 2200277.
37. Cao L., Pizzi A., Zhang Q., et al. Preparation and Characterization of a Novel Environment-Friendly Urea-Glyoxal Resin of Improved Bonding Performance. *J. European Polymer Journal*. 2022, 162: 110915.
38. Xu Y., Xu Y., Han Y., et al. The Effect of Enzymolysis on Performance of Soy Protein-Based Adhesive. *J. Molecules*. 2018, 23(11): 2752.